MONTHLY NOTICES of the Royal Astronomical Society

Flare QPPs in AB Dor: I. Identical scaling laws to solar and stellar flares and clues of magnetoacoustic waves

Journal:	*Monthly Notices of the Royal Astronomical Society*
Manuscript ID	Draft
Manuscript type:	Main Journal
Date Submitted by the Author:	n/a
Complete List of Authors:	Kalugodu, Chandrashekhar; University of Oslo, Srivastava, Abhishek; IIT BHU, Department of Physics Banerjee, Dipankar; Aryabhatta Research Institute of Observational Sciences Pandey, Jeewan; Aryabhatta Research Institute of Observational Sciences, ; Karmakar, Subhajeet; Monterey Institute for Research in Astronomy, Astronomy & Astrophysics Nakariakov, Valery; University of Warwick,
Keywords:	stars: coronae < Stars, stars: individual:... < Stars, stars: solar-type < Stars, stars: flare < Stars, stars: oscillations (including pulsations) < Stars

MNRAS **000**, 000–000 (2021) Preprint 22 September 2021 Compiled using MNRAS LATEX style file v3.0

Flare QPPs in AB Dor: I. Identical scaling laws to solar and stellar flares and clues of magnetoacoustic waves

K. Chandrashekhar,[1,2]★, A.K. Srivastava[3], D. Banerjee[4,5,6], J.C. Pandey[4], S. Karmakar[7], and V.M. Nakariakov[8,9]

[1]*Rosseland Centre for Solar Physics, University of Oslo, P.O. Box 1029 Blindern, N-0315 Oslo, Norway*
[2]*Institute of Theoretical Astrophysics, University of Oslo, P.O. Box 1029 Blindern, N-0315 Oslo, Norway*
[3]*Department of Physics, Indian Institute of Technology (BHU), Varanasi-221005, India*
[4] *Aryabhatta Research Institute of Observational Sciences (ARIES), Manora Peak, Nainital-263 002, India*
[5]*Indian Institute of Astrophysics, 2nd Block Koramangala, Bangalore 560034, India*
[6]*Center of Excellence in Space Science, IISER Kolkata, Kolkata 741246, India*
[7] *Monterey Institute for Research in Astronomy (MIRA) 200 8th Street, Marina California - 93933, USA*
[8] *Centre for Fusion, Space and Astrophysics, Department of Physics, University of Warwick, Coventry CV4 7AL, UK*
[9] *St. Petersburg Branch, Special Astrophysical Observatory, Russian Academy of Sciences, St. Petersburg, Russia*

Accepted XXX. Received YYY; in original form ZZZ

ABSTRACT

Quasi-periodic pulsations (QPP) in the soft X-ray light curves produced by seven flares on an active rapidly rotating K0 dwarf AB Dor observed with the XMM-Newton satellite are studied. QPP which belong to the specific, monotonously-decaying quasi-harmonic class occurring in the thermal emission in the decay phase of the flare are considered. Oscillation periods and damping times of QPPs are 45.78 ± 26.40 min and 66.57 ± 42.00 , respectively. These values are longer than in previously determined for the same QPP class in solar and other stellar flares. The Kolmogorov–Smirnov test reveals that the QPPs in the AB Dor flares are similar to the previously reported solar and stellar QPPs. The scaling law of the AB Dor QPP damping times with the oscillation periods is 1.62 ± 0.72, and exhibits the same nature as observed in the flares at the Sun and other magnetically active solar-type stars. This implies that QPPs at AB Dor, belonging to the monotonously-decaying quasi-harmonic class may have a similar origin as in the Sun and other active stars. The physical mechanism for the detected QPP can be attributed to slow magnetoacoustic oscillations. To the best of our knowledge, the present findings are the first evidence of QPP of this class observed at AB Dor, and we discuss its physical implications in its stellar coronae.

Key words: stars: coronae – stars: individual (AB Dor) – stars: solar-type –stars: flare – stars: oscillations – X-rays: stars

1 INTRODUCTION

Quasi-repetitive patterns have been detected in light curves of solar and stellar flares at all electromagnetic wavelengths, from gamma-rays to the radio emission (e.g., Parks & Winckler 1969; Qin et al. 1996; Nakariakov et al. 2003; Wang et al. 2003a; Harrison 1987; Pandey & Srivastava 2009; Li & Gan 2008; Srivastava et al. 2018; Ning 2014; Nakariakov et al. 2010b; Pugh et al. 2016; Li et al. 2020). These are referred to as quasi-periodic pulsations (QPP, see Kupriyanova et al. 2020; Zimovets et al. 2021, for recent comprehensive reviews). Periodicities detected in QPP range from a fraction of a second to several tens of minutes (e.g. Aschwanden 1987; Nakariakov & Melnikov 2009; Van Doorsselaere et al. 2016). There have been several physical mechanisms for QPP, proposed in the literature (see McLaughlin et al. 2018; Zimovets et al. 2021, for reviews). Several mechanisms are based on magnetohydrodynamic (MHD) oscillations which can either induce repetitive magnetic reconnection (e.g., Chen & Priest 2006; Nakariakov et al. 2006), or be induced by spontaneous reconnection (e.g., Capettini et al. 2020; Miao et al. 2021). The task of attributing a QPP to a certain specific class, typical for a specific mechanism is an ongoing challenge (Nakariakov et al. 2019a). The recent Bayesian statistical analysis of white-light stellar flares revealed at least three distinct classes of QPP, characterised by rapidly decaying harmonic oscillations, finite narrowband wave trains, and non-sinusoidal pulsations (Pascoe et al. 2020).

QPPs provide a promising tool for the diagnostics of flaring plasmas and physical processes operating in them via the method of MHD seismology (e.g., De Moortel & Nakariakov 2012; McLaughlin et al. 2018; Nakariakov & Kolotkov 2020, and refer-

★ E-mail: chandrashekhar.kalugodu@astro.uio.no

ences therein). Associating QPPs with a specific, MHD-wave-based mechanism allows us to relate observable parameters of QPPs, i.e., periods, amplitudes, and damping times with observable morphological and plasma parameters of the flaring active regions, e.g., lengths and widths of coronal loops and arcades, and temperature and density. In turn, those derived parameters could deliver important and often unique information about the magnetic field strength, density scale height, Alfvén speed, magnetic expansion, heating function, transport coefficients, fine sub-resolution structuring, etc. (e.g., Nakariakov & Ofman 2001; Srivastava et al. 2008; Andries et al. 2009; Srivastava & Dwivedi 2010; Wang 2011; Srivastava et al. 2013; Guo et al. 2015; Kolotkov et al. 2020, and references therein). Methods of the seismological diagnostics of the solar corona can be extended to stellar coronae, revealing their crucial physical properties (e.g., magnetic fields; Mitra-Kraev et al. 2005; Pandey & Srivastava 2009, and the references therein). In particular, there are advancements in determining characteristic physical properties, such as the density scale height, and clues of the magnetic expansion in stellar coronae, based on the observed MHD modes and related seismology (e.g., Srivastava & Dwivedi 2010; Doyle et al. 2018).

The evolution, propagation, and dissipation of magnetoacoustic waves in the magnetically structured coronae, causing QPPs, ought to be associated with certain scaling laws linking with each other various observables, such as the amplitudes, periods, damping times, quality factors and other characteristic features of the signals. Such scaling laws provide not only the clues about the wave behaviour but also inference about physical properties of the medium (e.g., Aschwanden et al. 2008; Cho et al. 2016). Obviously, such scaling laws should be determined for QPP of a certain class, i.e., which are associated with a specific mechanism or at least have specific distinct empirical signatures. One such class comprises monotonously-decaying quasi-harmonic oscillations of thermal emission in the decay phase of a flare, which are associated with slow magnetoacoustic oscillations (e.g., Nakariakov et al. 2019b; Wang et al. 2021, and references therein). Effective excitation of slow magnetoacoustic oscillations in a flaring loop has been numerically demonstrated by Reale et al. (2018, 2019). QPP of this class appear in the decay phase of a flare as a rapidly decaying almost harmonic modulation of thermal emission, on both the Sun (e.g., Kim et al. 2012) and stars (e.g., Doyle et al. 2018; Broomhall et al. 2019). In particular, Anfinogentov et al. (2013) have detected a monotonously-decaying harmonic QPP with the period of about 32 min and decay time 46 min on the dM4.5e star YZ CMi. Srivastava et al. (2013) have identified 1261 s and 687 s QPPs in the decay phase of a flare on Proxima Centauri in the soft (0.3–10.0 keV) X-ray energy band, and interpreted them as two harmonics of a slow magnetoacoustic wave excited in a stellar coronal loop. Another example of the co-existence of monotonously-decaying harmonic QPPs with two different periods, about 78 min and 32 min, on a white-light flare on the star KIC 9655129 has been found by Pugh et al. (2015). (Pugh et al. 2016) presented 11 white light stellar flares with pronounced QPP of this class. Broomhall et al. (2019) have detected a QPP pattern resembling a slow oscillation during a flare decay on a similar star EK Dra in the soft X-ray energy band and inferred the origin of the observed QPP as a modulation of X-ray emissions due to the motion of flare generated charged particles. For flares observed in soft X-rays, the QPPs periodicities discovered in solar flares are an order of magnitude shorter compared to those detected in stellar flares (Cho et al. 2016).

In this paper, we study monotonously-decaying quasi-harmonic QPPs of thermal emission during the decay phase of several flares observed on the highly active K0 dwarf AB Dor, for the first time. AB Dor is a quadruple system and the brightest star of this quadruple system. AB Dor A (hereafter AB Dor) is a well known, closest ultra-fast rotator (rotational period = 0.51 d, distance = 15.3 pc; Pakull 1981; Guirado et al. 1997, 2011) and has one of the brightest coronal X-ray source. AB Dor with its ultra fast rotation exhibits a high level of magnetic activity phenomena such as flares (e.g. Järvinen et al. 2005; Cohen et al. 2010; Schmitt et al. 2019). AB Dor shows a highly variable coronal X-ray emission which is attributed to frequent flaring events on time scales from minutes to hours (Vilhu et al. 1993; Güdel et al. 2001; Lalitha & Schmitt 2013). We have estimated the periods and damping times of soft X-ray QPPs detected in flares on AB Dor, and compared their properties with solar, and previously reported stellar cases (Cho et al. 2016). We confirm that the derived scaling law established for the AB Dor flares QPP of the slow magnetoacoustic class is similar to the Sun and other flaring Sun-like stars. We provide the physical significance of the derived scaling law in the context of AB Dor flares in respect to stellar corona. In Sect. 2, we discuss in detail the Observations and Data Reduction. The observational results are presented in Sect. 3. The last section is devoted to the Discussion and Conclusions.

2 OBSERVATIONS AND DATA REDUCTION

AB Dor has been frequently observed in last several years by the XMM-Newton satellite (Jansen et al. 2001) using the European Photon Imaging Camera (EPIC; Turner et al. 2001; Strüder et al. 2001) and Reflection Grating Spectrometer (RGS; den Herder et al. 2001) instruments. The EPIC comprises of three CCDs as the backend of three X-ray telescopes: a p-n junction (PN) CCD, and two identical metal oxide semiconductor (MOS) CCDs, MOS1 and MOS2. The EPIC has the energy range of 0.15–15 keV, spatial resolution of 4.5–6.6 arcsec, and the relative spectral resolution ($E/\Delta E$) of 20–50. The RGS is composed of two identical grating spectrometers RGS1 and RGS2. The dispersed photons are recorded by a strip of eight CCD MOS chips. It covers the energy range of a 0.3–2.5 keV with a spectral resolution of 0.05 Å and area of about 140 cm^2 at 15 Å.

The log of the observations used in our study is given in Table 1. A total of 40 observations were made by XMM-Newton from 2000 to 2012. In one occasion (observation ID 0123720101) data is not available in the archive, in four occasions (observation ID: 0134520601, 0134520501, 0160363101, and 0160363301), the filter was closed during the observations. Therefore, we left only with 35 observations, which were analysed in the present study. In our analysis, we account a single revolution as a single set, which gives a total of 31 sets combining those 35 observations. The nomenclature of the sets is given as Sij, where ij = 01, 02, ..., 31, (see the first three columns of Table 1 for further details). Among 31 sets, 11 sets were obtained with all PN, MOS and RGS, 2 sets with PN and RGS, 8 sets with MOS and RGS, and the remaining 10 sets with RGS only. Exposure times varied from ~4 ks to ~63 ks (see column 5). In total, AB Dor was observed for 33 ks by the PN detector and 427 ks by MOS detectors and ~1583 ks by RGS detector.

The data obtained with EPIC and RGS instruments were reduced using the Science Analysis System (SAS) software, version 17.0.0 of XMM-Newton with the updated calibration files. The EPIC event files were generated using the EPCHAIN and EMCHAIN tasks. Due to the background contribution at high energies, we have limited our analysis to the 0.3–10.0 keV energy band for EPIC observations. Both MOS and PN event list files were extracted using the SAS task EVSELECT. X-ray light curves from the

EPIC observations were generated from on-source counts obtained from circular regions with a radius of 36 arcsec around the source. The background was chosen from source-free regions on the detectors surrounding the source. Finally the EPIC light curves were corrected for the background contribution and other effects using the tasks EPICLCCORR. The RGS data were processed by using the task RGSPROC for the source coordinates of AB Dor. A banana plot was created for each observation ID using the task EVSELECT in order to verify the RGS field of view, and checking whether the source regions of the prime source AB Dor is centered correctly. The background-subtracted and dead time corrected combined light curves of RGS instruments (RGS1 + RGS2) with both the orders (order 1 and 2) were generated using the SAS task RGSLCCOR. We have removed from our analysis the part of the light curve which was found to be affected by a high background proton flare and having a background count rate > 0.4 cts.

3 ANALYSIS AND RESULTS

For the analysis, light curves of the decay phases of the flares were selected manually in each of the flare events. The decay phase covers the time interval from the maximum emission time up to when the count rate is approximately equal to the quiescent part of the count rate. The left panel of Figure 1 shows the X-ray light curve of AB Dor for data set 1, where the green part in the light curve is selected for our analysis. Decay phases of light curves are analyzed using the Empirical Mode Decomposition method (EMD; Huang et al. 1998; Huang & Wu 2008). EMD decomposes a signal into a set of intrinsic mode functions (IMFs). An IMF represents an oscillation present in the signal. An IMF is not necessarily a harmonic signal, i.e., the amplitude, frequency and phase of the oscillation can vary in time (see Kolotkov et al. 2015, for discussion). IMFs are obtained by the sifting process, that is by subtracting an average envelope signal from the original signal and defining the resultant signal as a new time series. In the next step, the new time series is considered as an original signal, and the process is repeated until the number of extrema becomes equal to the number of zero-crossings. Highest-frequency oscillations are filtered in the first of the IMFs. Subsequent IMFs contain lower frequency oscillations in the descending order. The last IMFs can be considered as the lowest-frequency oscillation or a background trend. Also, the trend could be obtained by summing up two or three lowest frequency IMFs. In the example shown in Figure 1, the right bottom panel shows the analysed part of the light curve in the black colour, and the superimposed yellow colour line is the background trend determined from the lowest frequency IMFs. The background trend subtracted light curve is correlated with the IMFs obtained. In this study we are interested in IMFs which resemble decaying harmonic oscillations, i.e., which could belong to the specific QPP class that is associated with slow magnetoacoustic oscillations. The IMF of this kind, with the best correlation is used for determining the period and damping time of the QPP. The right top panel in Figure 1 shows the background-trend subtracted light curve in black, along with the best correlated IMF in red. In order to determine the damping time, the best estimated IMF was fitted with a damped sine (DS) curve,

$$F(t) = A \exp\left(-\frac{t}{\tau}\right) \sin\left(\frac{2\pi t}{P} - \phi\right), \quad (1)$$

where P is the oscillation period, A is amplitude, ϕ is the phase, and τ the damping time. An example of a such an IMF and its best-fitting by Eq. (1) is shown by the blue colour in the right top panel of Figure 1. There is no an exact agreement between an IMF and the best-fitting decaying sinusoidal curve because of the non-stationary, and hence, non-harmonic nature of the IMF. However, such a fit allows us to estimate roughly the oscillation period and the damping time.

A total of 16 flare events with QPPs in the decay phases of the analysed flares are identified. A few flare events are registered with more than one detector filter. Also, we note that we have two flares with QPPs identified in three data sets (S01, S16 and S23). Table 2 shows the values of periods and damping times for all QPPs detected in our data. We have detected 6 QPPs in the signals recorded with the PN detector, 6 QPPs with the MOS detector, and 15 QPPs with the RGS detector. Finally, out of 27 QPP events, we selected 8 QPP events that apparently belonged to the monotonously-decaying harmonic oscillatory QPP class (i.e., those which could be associated with slow oscillations) for further analysis. In Figure 2 we show all the QPP events of this specific class, detected in our study.

Figure 3 shows the scaling of damping times with oscillation periods determined for the QPP detected in this study, together with the QPP parameters obtained for solar and stellar flares by Cho et al. (2016). Histogram density plots of the QPP parameters obtained previously and in this study are constructed. The QPP periods of the flares on AB Dor are similar to those in the previously analysed stellar flares, with a few of them being even longer. In addition, logarithms of the data points are fitted by linear functions, i.e., were subject to the logarithmic linear regression, separately for the previously determined solar and stellar flares, for the AB Dor flares studied here, and also for all the data points together. The power-law indices obtained here for the AB Dor, and also previously for solar and stellar flares are found to be 0.73±0.11, 1.10±0.13, and 0.98±0.05, respectively, and 0.98±0.02 for all the events. All four scalings are rather similar to each other, giving roughly the linear dependence of the damping time with the oscillation period. In particular, it justifies the choice of the QPP events in the AB Dor flares, made in this study: not only the shape of the signals is similar to this in the previously studied solar and stellar flares, but also the scaling of the damping time with the oscillation period is linear too.

4 DISCUSSION AND CONCLUSIONS

We have analysed a total of 31 data sets which contained signatures of the flaring activity on AB Dor, observed from the year 2000 to 2012 by XMM-Newton. Out of these 31 data sets, a total of 13 data sets are identified with at least one flare event with QPP. In data sets S01, S16, and S23, we have identified two flare events with QPPs. A total of 16 unique flaring events with QPPs in the decay phase are identified and analyzed (see Table 2). We used the EMD method to identify different IMFs in those light curves. For the further analysis we selected seven IMFs which apparently belonged to the monotonously-decaying quasi-harmonic QPP class. Those IMFs were fitted with an exponentially damping sinusoidal function given by equation 1) to find the best-fitting period and damping time of the QPP. Average values of the oscillation period, damping time, and the ratio of the damping time to oscillation period are given in the table 3. We found that the average period of QPPs detected in AB Dor is 45.78 ± 26.40 minutes. This value is longer than the average oscillation periods of QPPs of the same class detected in solar (0.90 ± 0.56 minutes) and stellar flares (16.25 ± 15.86 minutes) by (Cho et al. 2016). Also, we found that the average damping times

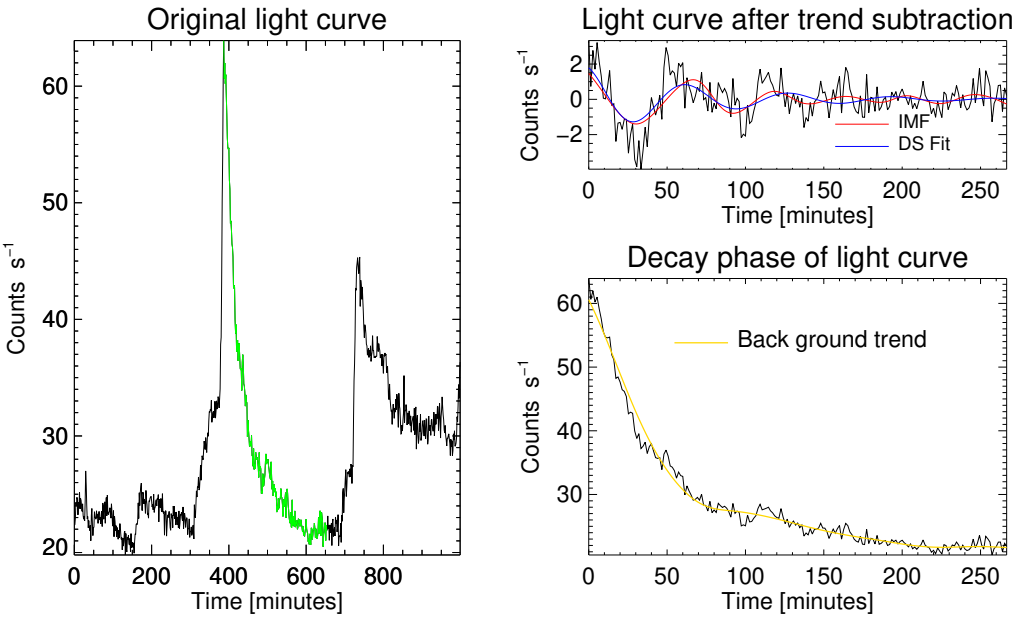

Figure 1. Results of the EMD analysis of a flaring signal in data set 1 obtained with the EPIC-PN detector. The left panel shows the original light curve with a 80 s bin. The part of the light curve in the green colour shows the decay-phase time interval selected for the analysis. The right lower panel shows the analysed light curve in black along with the background trend obtained with the EMD analysis, shown in yellow. The right top panel shows the light curve after the background trend subtraction, in black, the monotonously-decaying quasi-harmonic IMF in red, and the best-fitting exponentially-damped harmonic curve in blue.

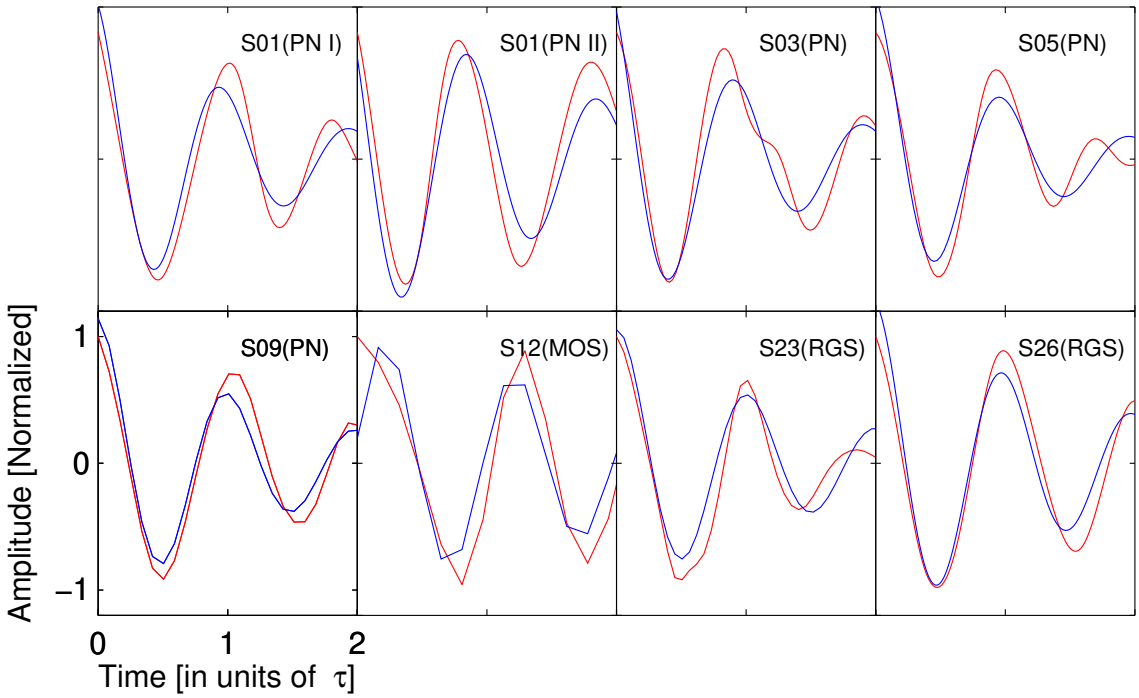

Figure 2. The monotonously-decaying quasi-harmonic IMF and the best-fitting exponentially-damped harmonic curves of the decay phases of X-ray flares on AB Dor. In each panel the best correlated IMF found in the detrended decay phase light curve is shown in the red colour, and the exponentially-damped sinusoidal function best-fitting the IMF is shown in blue. In each panel, the time axis is normalised to the damping time τ, and the vertical axis is normalized to the maximum amplitude of the QPP. Labels in each panel show the data set in which the flare event with QPP is identified. Roman letters I and II stand for the first and second flare events with the identified QPP in the same data set.

Table 1. The log of the analysed X-ray observations of AB Dor

Data set	Rev. –	Observation ID	Detector[1] (Filter[2])	Obs. Date (yyyy-mm-dd)	Time[3] (UT) (hh:mm:ss)	Exposure Time(s)	Off axis (′)
S01	72	0123720201	pn(me)	2000-05-01	02:52:31	60000	0.303
			RGS		02:30:21	62172	
S02	91	0126130201	PN(ME)	2000-06-07	09:44:12	41900	0.304
			RGS		05:29:46	59010	
S03	162	0123720301	PN(ME)	2000-10-27	15:23:55	55700	0.026
			M1(ME)		15:10:06	56039	
			M2(ME)		15:10:06	56039	
			RGS		15:01:40	58908	
S04a	185	0133120701	RGS	2000-12-11	14:38:38	58820	0.127
S04b	185	0133120101	RGS	2000-12-11	17:10:30	59420	0.127
S04c	185	0133120201	PN(TH)	2000-12-12	17:40:23	8497	2.211
			M1(TH)		20:22:00	6185	
			M2(TH)		20:22:00	6185	
			RGS		16:50:29	20909	
S05	205	0134520301	PN(ME)	2001-01-20	15:48:14	49100	0.132
			M1(ME)		15:34:37	49390	
			M2(ME)		15:34:37	49391	
			RGS		15:26:10	52309	
S06	266	0134520701	PN(ME)	2001-05-22	17:05:58	48219	0.275
			M1(ME)		16:50:15	49000	
			M2(ME)		16:50:15	49011	
			RGS		16:43:55	49610	
S07	338	0134521301	M1(ME)	2001-10-13	11:20:04	39147	0.110
			M2(ME)		11:20:04	39147	
			RGS		11:13:44	39745	
S08	375	0134521401	M1(ME)	2001-12-26	04:50:20	4200	0.156
			M2(ME)		04:50:20	4200	
			RGS		04:44:01	49732	
S09	429	0134521501	PN(ME)	2002-04-12	22:53:54	15932	0.175
			M1(ME)		22:34:35	16241	
			M2(ME)		22:34:37	16241	
			RGS		12:33:39	53220	
S10a	462	0155150101	PN(ME)	2002-06-18	03:12:38	5000	0.022
			M1(ME)		07:03:16	6084	
			M2(ME)		07:03:16	6084	
S10b	462	0134521601	PN(ME)	2002-06-18	16:49:58	17461	0.062
			M1(ME)		16:27:06	17117	
			M2(ME)		16:27:06	17117	
			RGS		09:30:06	47970	
S11	532	0134521801	RGS	2002-11-05	06:25:44	19912	0.159
S12	537	0134521701	M1(ME)	2002-11-15	05:45:10	19401	0.126
			M2(ME)		05:45:14	19652	
			RGS		05:44:24	19913	
S13	546	0134522001	M1(ME)	2002-12-03	05:00:00	18992	0.076
			M2(ME)		04:59:57	18992	
			RGS		04:59:07	20641	
S14	560	0134522101	M1(ME)	2002-12-30	10:49:02	48648	0.080
			M2(ME)		10:48:58	48400	
			RGS		10:48:08	50648	
S15	572	0134522201	RGS	2003-01-23	03:22:28	52368	0.086
S16	605	0134522301	M1(ME)	2003-03-30	20:19:57	3600	0.001
			M2(ME)		20:19:56	3600	
			RGS		10:30:52	48918	0.073
S17	636	0134522401	RGS	2003-05-31	16:39:30	28869	0.029
S18a	668	0160362501	M1(ME)	2003-08-02	10:05:29	5001	0.084
			M2(ME)		10:05:28	5001	
			RGS		05:13:56	22714	
S18b	668	0160362601	M1(ME)	2003-08-02	13:14:01	4999	0.118
			M2(ME)		13:14:01	4999	
			RGS		13:13:17	23919	
S19	709	0160362701	PN(TN)	2003-10-24	05:25:27	10400	0.110
			M1(ME)		03:22:56	17521	
			M2(ME)		03:22:56	17521	
			RGS		17:54:57	51836	
S20	732	0160362801	RGS	2003-12-08	01:44:24	53694	0.116
S21	910	0160362901	RGS	2004-11-27	20:14:10	56340	1.669
S22	981	0160363001	RGS	2005-04-18	09:35:17	52098	0.073
S23	1072	0160363201	RGS	2005-10-16	22:28:17	50099	0.097
S24	1293	0412580101	RGS	2006-12-31	20:30:18	45019	0.066
S25	1393	0412580201	RGS	2007-07-19	03:37:30	56973	0.108
S26	1478	0412580301	RGS	2008-01-03	19:26:09	48901	0.080
S27	1662	0412580401	PN(TH)	2009-01-05	06:28:06	10000	0.099
			M1(TH)		06:25:18	9990	
			M2(TH)		06:25:22	9990	
			RGS	2009-01-04	19:24:54	49875	
S28	1825	0602240201	PN(ME)	2009-11-25	21:00:10	55971	1.120
			M1(ME)		20:55:00	56103	
			M2(ME)		20:54:55	55856	
			RGS		20:53:43	58442	
S29	1848	0412580601	PN(TH)	2010-01-12	00:56:59	10000	0.029
			M1(TH)		00:54:10	9990	
			M2(TH)		00:54:15	9990	
			RGS	2010-01-11	13:53:04	49917	
S30	2027	0412580701	PN(TH)	2011-01-03	02:10:27	10000	0.107
			M1(TH)		02:07:20	12287	
			M2(TH)		02:07:19	12292	
			RGS	2011-01-02	15:05:24	62871	
S31	2209	0412580801	M1(TH)	2012-01-01	02:06:59	9999	0.001
			M2(TH)		02:06:59	10000	
			RGS	2011-12-31	15:23:24	61874	

[1] M1 and M2 stand for MOS1 and MOS2, respectively.
[2] TH, ME and TN stand for thick, medium and thin filters, respectively.
[3] Exposure start time.

Table 2. The monotonously-decaying quasi-harmonic EMD and the best-fitting exponentially-damped harmonic QPP detected in the decay phases of X-ray flares on AB Dor. S. The number in column 1 stands for the serial number of the flaring event. Columns two, three, and four are the data set, observation ID, and detector/filter, respectively same as in Table 1. Columns five and six are the oscillation period and damping times of the QPPs detected, in minutes. In data sets S01, S16, and S23 we identified two flare events with QPP.

S. No	Data set	Observation ID	Detector (Filter)	P (minutes)	τ_d (minutes)
1	S01	0123720101	PN I[4]	65.8 ± 1.3	76.7±11.2
			RGS I	59.0 ± 4.0	81.3 ± 51.6
2	S01	0123720101	PN II[5]	68.3 ± 1.0	123.5 ± 22.4
			RGS II	95.2 ± 6.3	216.2± 242.2
3	S03	0123720301	MOS	69.5 ± 2.6	78.0 ± 23.8
			PN	55.4 ± 0.6	66.4 ± 5.7
			RGS	59.8 ± 7.6	52.8 ± 41.9
4	S05	0134520301	MOS	39.4 ± 3.6	130.8± 239.8
			PN	50.5 ± 1.4	50.4 ± 8.5
			RGS	67.8 ± 8.2	88.2 ± 102.3
5	S09	0134521501	MOS	12.4 ± 2.5	14.4 ± 18.5
			PN	15.9 ± 0.8	21.8 ± 8.1
6	S12	0134521701	MOS	8.2 ± 0.3	26.9 ± 21.9
			RGS	20.5 ± 1.8	37.6 ± 41.6
7	S14	0134522101	MOS	18.4 ± 0.5	117.1 ± 100.2
			RGS	16.0 ± 1.9	45.5 ± 97.4
8	S16	0134522301	RGS I	54.9 ± 5.5	61.4 ± 37.0
9	S16	0134522301	RGS II	44.6 ± 5.9	35.3 ± 27.0
10	S20	0160362801	RGS	93.6 ± 5.7	137.5 ± 86.8
11	S22	0160363001	RGS	9.6 ± 2.9	23.1 ± 101.8
12	S23	0160363201	RGS I	23.7 ± 5.4	35.5 ± 68.2
13	S23	0160363201	RGS II	9.2 ± 2.6	27.7 ± 138.4
14	S25	0412580201	RGS	10.4 ± 3.1	2809.3 ± 137349
15	S26	0412580301	RGS	78.4 ± 2.3	131.4 ± 40.0
16	S28	0602240201	MOS	156.3 ± 0.6	36159.7 ± 175836.0
			RGS	159.8 ± 6.0	262.8 ± 107.8
			PN	103.9± 0.3	761.4 ± 114.2

[4] I refers to the first flare event with QPP in the data set.
[5] II refers to the second flare event with QPP in the data set.

Table 3. Statistics of oscillation periods and damping times of monotonously-decaying quasi-harmonic QPP studied by Cho et al. (2016), and determined in decay phases of X-ray flares on AB Dor. The p-values of the K-S test are determined for the corresponding previously established solar and stellar distributions separately with the AB Dor QPP studied here.

Parameters	Solar QPP	Stellar QPP	AB Dor QPP
Average P (minutes)	0.90 ± 0.56	16.25 ± 15.88	45.78 ± 26.40
Average τ (minutes)	1.53 ± 1.10	27.18 ± 28.72	66.57 ± 42.00
τ/P	1.74 ± 0.77	1.69 ± 0.56	1.62 ± 0.72
K-S test p-value	0.73	0.74	–

of the QPPs for AB Dor flares is 66.57 ± 42.00 minutes. This value is also longer than the damping times found for solar (1.53 ± 1.10 minutes) and stellar (27.18 ± 28.72 minutes) QPPs by Cho et al. (2016). But the ratio of damping time to the period of the QPPs found in AB Dor flares 1.62 ± 0.72 is similar to that found previously for solar (1.74 ± 0.77) and stellar (1.69 ± 0.56) QPPs. All three sets of QPP show a similar almost-linear dependence of the damping time on oscillation period. The slope of the dependence established for AB Dor is slightly flatter than for the solar and stellar flares, while this discrepancy could be attributed to the insufficient number of data points.

A statistical Kolmogorov–Smirnov (K-S) test is performed to determine quantitatively whether analysed parameters belong to the same distribution or not. The K-S test is done for combinations of the previously studied distributions of τ/P values separately for solar QPPs versus AB Dor QPPs and stellar QPPs, versus AB Dor QPPs. The p-values of the K-S test are 0.73 and 0.74 respectively for solar and stellar when compared with AB Dor τ/P values (see Table 3. A small p-value (e.g., 0.01) would indicate that the cumulative distributions are significantly different from each other. However, the obtained values suggest that those three distributions of τ/P are similar. The almost matched scaling-laws between damping times and oscillation periods of monotonously-decaying quasi-harmonic QPP occurring the decay phases of solar and stellar X-ray flares could indicate the similarity of underlying physical processes responsible for the QPP.

Thus, the scaling of the damping times with the oscillation periods of the monotonously-decaying quasi-harmonic QPP observed previously in the decay phases of solar and stellar flares by Cho et al. (2016) and in the present study for AB Dor can be fitted with a power-law dependence with the index of 0.98±0.02. A similar scaling has been established for rapidly-decaying harmonic oscillations of the Doppler shift of the emission lines associated with a hot plasma, known as SUMER oscillations, detected in spectroscopic

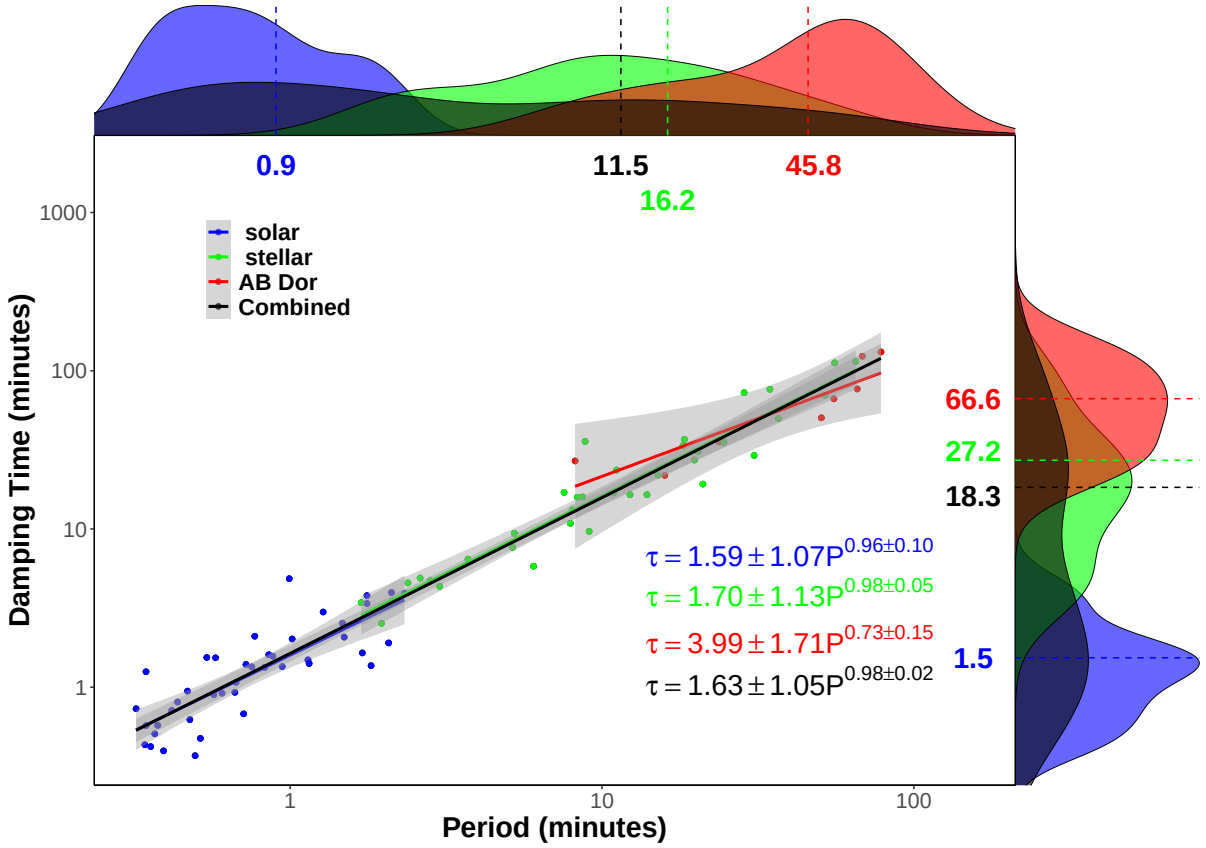

Figure 3. Oscillation periods versus damping times of monotonously-decaying quasi-harmonic QPP occurring the decay phases of solar and stellar flares in the X-ray emission. Blue and green colour filled circles represent data for solar and stellar flares, respectively, as studied by Cho et al. (2016). Red filled circles represent data points for AB Dor QPPs studied here. Solid colour lines are the logarithmic linear regression fits to the data points, corresponding to the respective sets of flares. The grey shaded area around the solid lines of different colours is the 1 σ confidence band for respective regression fits. The best fitting parameters are given by the text of the respective colours. The black solid line represents a linear fit of all the data points combined. Histogram density plots for damping time and period are shown along the right and top borders of the plot. Dash coloured lines on the histograms correspond to mean values of the damping time and periods, respectively. Corresponding values of the mean damping time and mean period are printed near the dashed lines.

observations of solar flares (Wang et al. 2003b; Verwichte et al. 2008). Similar oscillations have been detected in the microwave band (Kim et al. 2012). The damping of so-called sloshing oscillations, detected in imaging observations of solar flares, has a similar dependence on the oscillation period too (Nakariakov et al. 2010a). Both SUMER and sloshing oscillations are interpreted as slow magnetoacoustic oscillations, and it is likely that QPP detected in the AB Dor flares are linked with slow magnetoacoustic oscillations too. The oscillation period is determined by the length of the oscillating loop, divided by the sound speed which in turn depends on the square root of the plasma temperature. The flare peak temperature on AB Dor is approximately 5–10 times more than that of the flare peak temperature of the Sun (see Lalitha 2015). Thus we infer that the longer periods observed in AB Dor QPPs could be due to the longer loop lengths, because of the high magnetic activity of the star.

Another interpretation of the observed QPP could be connected with kink oscillations of the loops, i.e., standing fast magnetoacoustic waves. Kink oscillations which are often detected in solar active regions, show similar linear scaling of the damping time with oscillation period. Ofman & Wang (2002) found the power index as 1.07±0.16 in a set of 35 kink oscillations observed in the EUV band in the solar corona. A more comprehensive study of 223 kink oscillations by Nechaeva et al. (2019) confirmed the linear scaling of the damping time and oscillation period. The kink oscillation period is determined, by the order of magnitude, by the ratio of the loop length to the Alfvén speed. Thus, the same values of periods of kink oscillations would require much longer loops than in the case of slow oscillations, as the coronal plasma parameter β connected with the squares ratio of the sound and Alfvén speeds is lower than unity.

To the best of our knowledge, the present findings are the first evidence of the MHD wave generated QPPs observed in the flaring epochs of AB Dor. Although, our observational baseline does not permit in differentiating the slow and fast magnetoacoustic modes in the structured flaring loops of AB Dor. Moreover, the more flat linear behaviour of damping-time vs oscillation period with lesser slope compared to solar and other stellar flares could suggest that dissipation mechanism(s) might work in a different manner in the flaring loops of AB Dor. However, the discussion of the specific behaviour of the damping mechanism is out of the scope of this paper. We leave herewith these two important questions for the future potential works, while we complement that AB Dor flaring regions are almost behaving like solar and other stellar flares. Therefore, with these new results, we leap one more step ahead in unifying the physical behaviour of solar and stellar flares.

ACKNOWLEDGEMENTS

This work is supported by the BRICS Multilateral Research and Development Projects-2016 (DST/MRCK/BRICS/PilotCall1/Superflares/2017), project 'Superflares on stars and the Sun' and the Russian Foundation for Basic Research under grant 17-52-80064 BRICS-A. KC is supported by the Research Council of Norway through its Centres of Excellence scheme (project number 262622). VMN acknowledges, in the interpretation part, the support of the Russian Scientific Foundation grant 21-12-00195.

REFERENCES

Andries J., van Doorsselaere T., Roberts B., Verth G., Verwichte E., Erdélyi R., 2009, Space Sci. Rev., 149, 3
Anfinogentov S., Nakariakov V. M., Mathioudakis M., Van Doorsselaere T., Kowalski A. F., 2013, ApJ, 773, 156
Aschwanden M. J., 1987, Sol. Phys., 111, 113
Aschwanden M. J., Stern R. A., Güdel M., 2008, ApJ, 672, 659
Broomhall A. M., Thomas A. E. L., Pugh C. E., Pye J. P., Rosen S. R., 2019, A&A, 629, A147
Capettini H., Cécere M., Costa A., Krause G., Reula O., 2020, A&A, 644, A106
Chen P. F., Priest E. R., 2006, Sol. Phys., 238, 313
Cho I. H., Cho K. S., Nakariakov V. M., Kim S., Kumar P., 2016, ApJ, 830, 110
Cohen O., Drake J. J., Kashyap V. L., Hussain G. A. J., Gombosi T. I., 2010, ApJ, 721, 80
De Moortel I., Nakariakov V. M., 2012, Philosophical Transactions of the Royal Society of London Series A, 370, 3193
Doyle J. G., et al., 2018, MNRAS, 475, 2842
Güdel M., et al., 2001, A&A, 365, L336
Guirado J. C., et al., 1997, ApJ, 490, 835
Guirado J. C., Marcaide J. M., Martí-Vidal I., Le Bouquin J. B., Close L. M., Cotton W. D., Montalbán J., 2011, A&A, 533, A106
Guo Y., Erdélyi R., Srivastava A. K., Hao Q., Cheng X., Chen P. F., Ding M. D., Dwivedi B. N., 2015, ApJ, 799, 151
Harrison R. A., 1987, A&A, 182, 337
Huang N. E., Wu Z., 2008, Reviews of Geophysics, 46, RG2006
Huang N. E., et al., 1998, Proceedings of the Royal Society of London A: Mathematical, Physical and Engineering Sciences, 454, 903
Jansen F., et al., 2001, A&A, 365, L1
Järvinen S. P., Berdyugina S. V., Tuominen I., Cutispoto G., Bos M., 2005, A&A, 432, 657
Kim S., Nakariakov V. M., Shibasaki K., 2012, ApJ, 756, L36
Kolotkov D. Y., Nakariakov V. M., Kupriyanova E. G., Ratcliffe H., Shibasaki K., 2015, A&A, 574, A53
Kolotkov D. Y., Duckenfield T. J., Nakariakov V. M., 2020, A&A, 644, A33
Kupriyanova E., Kolotkov D., Nakariakov V., Kaufman A., 2020, Solar-Terrestrial Physics, 6, 3
Lalitha S., 2015, Proceedings of the International Astronomical Union, 11, 155–160
Lalitha S., Schmitt J. H. M. M., 2013, A&A, 559, A119
Li Y. P., Gan W. Q., 2008, Sol. Phys., 247, 77
Li D., Kolotkov D. Y., Nakariakov V. M., Lu L., Ning Z. J., 2020, ApJ, 888, 53
McLaughlin J. A., Nakariakov V. M., Dominique M., Jelínek P., Takasao S., 2018, Space Sci. Rev., 214, 45
Miao Y., Li D., Yuan D., Jiang C., Elmhamdi A., Zhao M., Anfinogentov S., 2021, ApJ, 908, L37
Mitra-Kraev U., Harra L. K., Williams D. R., Kraev E., 2005, A&A, 436, 1041
Nakariakov V. M., Kolotkov D. Y., 2020, ARA&A, 58, 441
Nakariakov V. M., Melnikov V. F., 2009, Space Sci. Rev., 149, 119
Nakariakov V. M., Ofman L., 2001, A&A, 372, L53
Nakariakov V. M., Melnikov V. F., Reznikova V. E., 2003, A&A, 412, L7
Nakariakov V. M., Foullon C., Verwichte E., Young N. P., 2006, A&A, 452, 343
Nakariakov V. M., Inglis A. R., Zimovets I. V., Foullon C., Verwichte E., Sych R., Myagkova I. N., 2010a, Plasma Physics and Controlled Fusion, 52, 124009
Nakariakov V. M., Foullon C., Myagkova I. N., Inglis A. R., 2010b, ApJ, 708, L47
Nakariakov V. M., Kolotkov D. Y., Kupriyanova E. G., Mehta T., Pugh C. E., Lee D. H., Broomhall A. M., 2019a, Plasma Physics and Controlled Fusion, 61, 014024
Nakariakov V. M., Kosak M. K., Kolotkov D. Y., Anfinogentov S. A., Kumar P., Moon Y. J., 2019b, ApJ, 874, L1
Nechaeva A., Zimovets I. V., Nakariakov V. M., Goddard C. R., 2019, ApJS, 241, 31
Ning Z., 2014, Sol. Phys., 289, 1239
Ofman L., Wang T., 2002, ApJ, 580, L85
Pakull M. W., 1981, A&A, 104, 33
Pandey J. C., Srivastava A. K., 2009, ApJ, 697, L153
Parks G. K., Winckler J. R., 1969, ApJ, 155, L117
Pascoe D. J., Smyrli A., Van Doorsselaere T., Broomhall A. M., 2020, ApJ, 905, 70
Pugh C. E., Nakariakov V. M., Broomhall A. M., 2015, ApJ, 813, L5
Pugh C. E., Armstrong D. J., Nakariakov V. M., Broomhall A. M., 2016, MNRAS, 459, 3659
Qin Z., Li C., Fu Q., Gao Z., 1996, Sol. Phys., 163, 383
Reale F., Lopez-Santiago J., Flaccomio E., Petralia A., Sciortino S., 2018, ApJ, 856, 51
Reale F., Testa P., Petralia A., Kolotkov D. Y., 2019, ApJ, 884, 131
Schmitt J. H. M. M., Ioannidis P., Robrade J., Czesla S., Schneider P. C., 2019, A&A, 628, A79
Srivastava A. K., Dwivedi B. N., 2010, New Astron., 15, 8
Srivastava A. K., Zaqarashvili T. V., Uddin W., Dwivedi B. N., Kumar P., 2008, MNRAS, 388, 1899
Srivastava A. K., Lalitha S., Pandey J. C., 2013, ApJ, 778, L28
Srivastava A. K., et al., 2018, arXiv e-prints,
Strüder L., et al., 2001, A&A, 365, L18
Turner M. J. L., et al., 2001, A&A, 365, L27
Van Doorsselaere T., Kupriyanova E. G., Yuan D., 2016, Sol. Phys., 291, 3143
Verwichte E., Haynes M., Arber T. D., Brady C. S., 2008, ApJ, 685, 1286
Vilhu O., Tsuru T., Collier Cameron A., Budding E., Banks T., Slee B., Ehrenfreund P., Foing B. H., 1993, A&A, 278, 467
Wang T., 2011, Space Sci. Rev., 158, 397
Wang T. J., Solanki S. K., Innes D. E., Curdt W., Marsch E., 2003a, A&A, 402, L17
Wang T. J., Solanki S. K., Curdt W., Innes D. E., Dammasch I. E., Kliem B., 2003b, A&A, 406, 1105
Wang T., Ofman L., Yuan D., Reale F., Kolotkov D. Y., Srivastava A. K., 2021, Space Sci. Rev., 217, 34
Zimovets I. V., et al., 2021, Space Sci. Rev., 217, 66
den Herder J. W., et al., 2001, A&A, 365, L7